

Parameter Space Exploration Reveals Interesting Mn-doped SrTiO₃ Structures

Gil M. Repa and Lisa A. Fredin
Department of Chemistry
Lehigh University, PA 18015, USA

July 22, 2021

The xyz coordinates of each optimized structure are https://github.com/fredingroup/Mn_V_STO.

Table of Contents

Figure S1: Perovskite Structure with A- and B-cells highlighted	3
Table S1: K-Grids for Full Band Structures	3
Table S2: Average wall times per atom	3
Figure S2: Location of defect in single vacancy supercells	4
Figure S3: Location of defect in double vacancies supercells	5
Figure S4: Location of defect in Mn doped supercells	6
Figure S5: Single point energy wall times with HSE06	7
Table S3: Final Energy/Atom from BLYP SCF Optimizations (eV)	8
Table S4: BLYP Formation Energies (eV)	9
Table S5: HSE06 Energy Per Atom (eV)	10
Table S6: Coordination Number	10
Table S7: Atomic identities at high symmetry points in supercells	11
Figure S6: 444vsro rotations	12
Figure S7: Single bond length distribution	13
Figure S8: Double bond length distribution	14
Figure S9: Single Mn-doped bond length distribution	15
Figure S10: Double Mn-doped bond length distribution	16
Figure S11: $3 \times 2 \times 2$ V_{Ti} - V_{Oz}	17
Figure S12: Mn^{2+} and Mn^{3+} geometries	17
Figure S13: Pure Supercells Bandstructures	18
Figure S14: V_O bandstructures	18
Figure S15: HSE06 band structures for asymmetric V_O defects.	19
Figure S16: BLYP band structures for A-site defects	20
Figure S17: BLYP band structures for $Mn^{2+/3+/4+}$ defects.	21
Figure S18: HSE06 predicted energy levels for V_{Ti} defects.	22
Figure S19: BLYP bands structures for $Mn^{2+/3+/4+}$ defects.	23
Figure S20: HSE06 predicted energy levels for asymmetric Mn-doped supercells	24

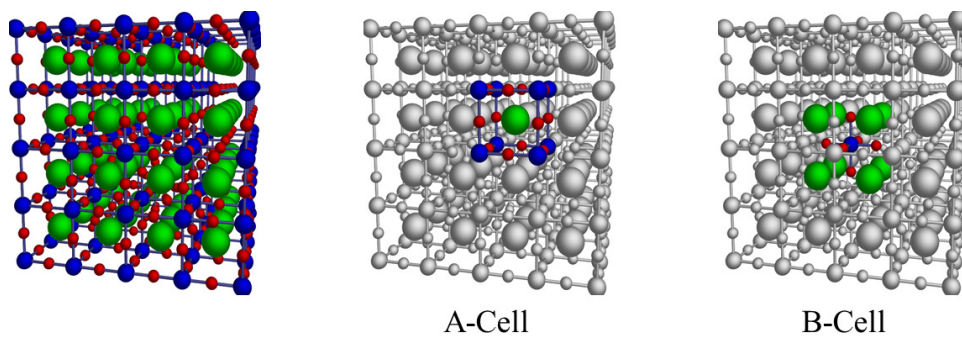


Fig. S1: Structure of SrTiO₃ with A- and B-cells highlighted.

Table S1: Size of K-Point grids used for BLYP band structure calculations

Supercell	K-Grid for SCF
222	4 x 4 x 4
322	6 x 4 x 4
333	3 x 3 x 3
334	4 x 4 x 6
444	4 x 4 x 4

Table S2: Average optimization time per atom (CPU-Hour/Atom) for BLYP Optimizations and HSE06 Single Point calculations.

Supercell	Optimization, BLYP	Single Point, HSE06
222	0.201	0.165
322	0.190	0.247
333	0.502	1.188
334	0.762	2.644
444	3.823	9.356

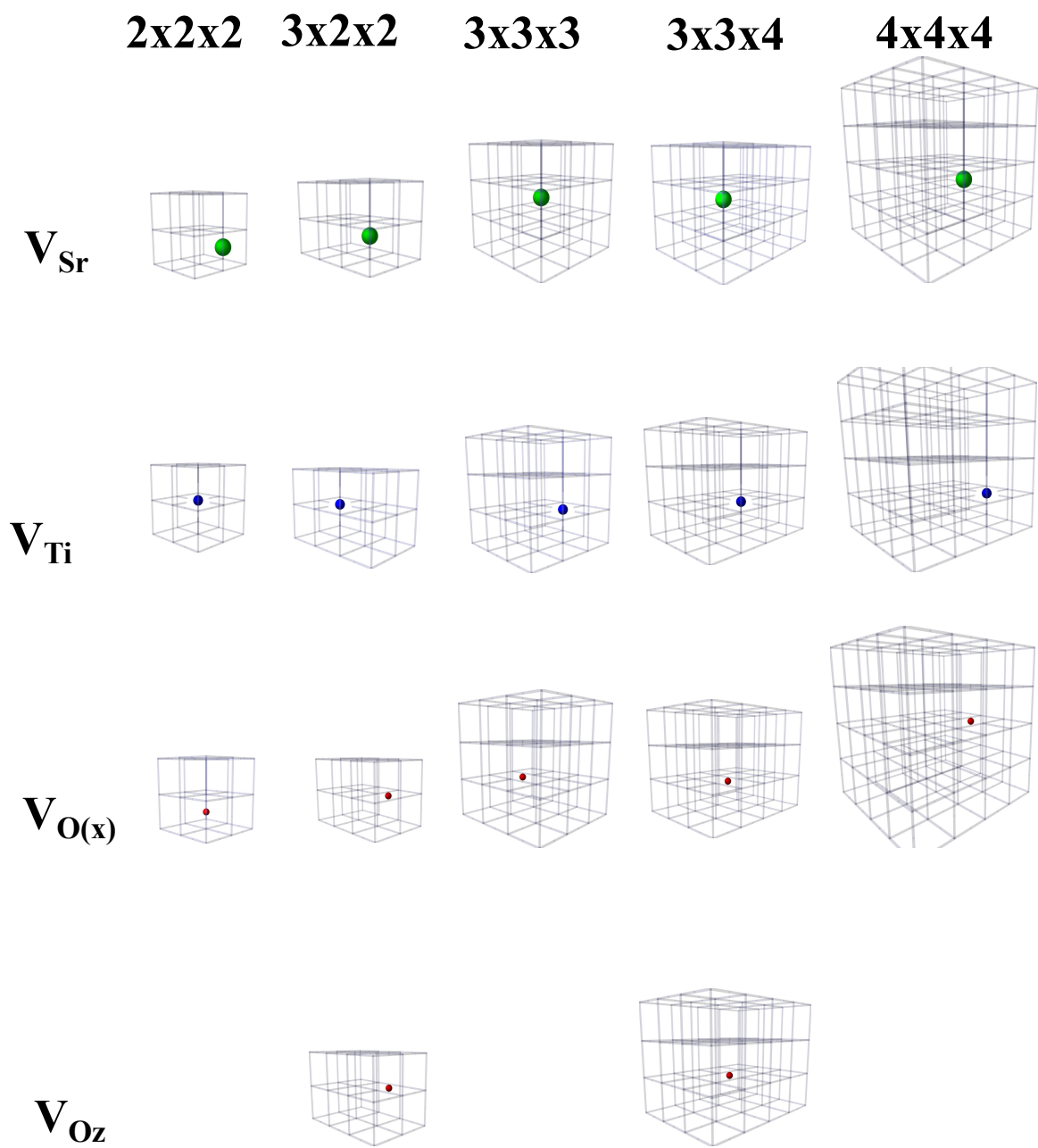


Fig. S2: Location of single vacancy after optimization with the BLYP functional in QuantumEspresso.

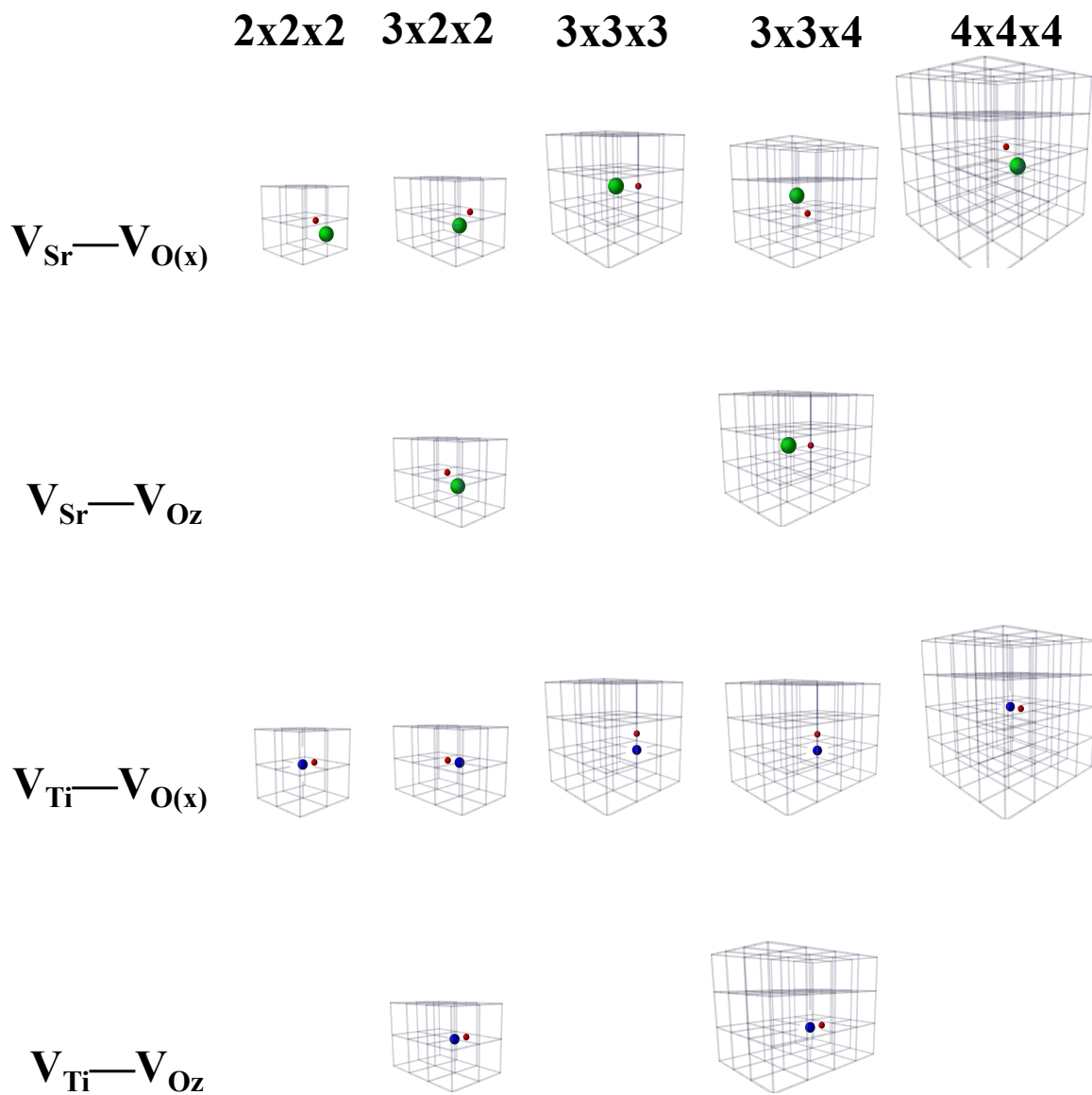


Fig. S3: Location of double vacancies after optimization with the BLYP functional in QuantumEspresso.

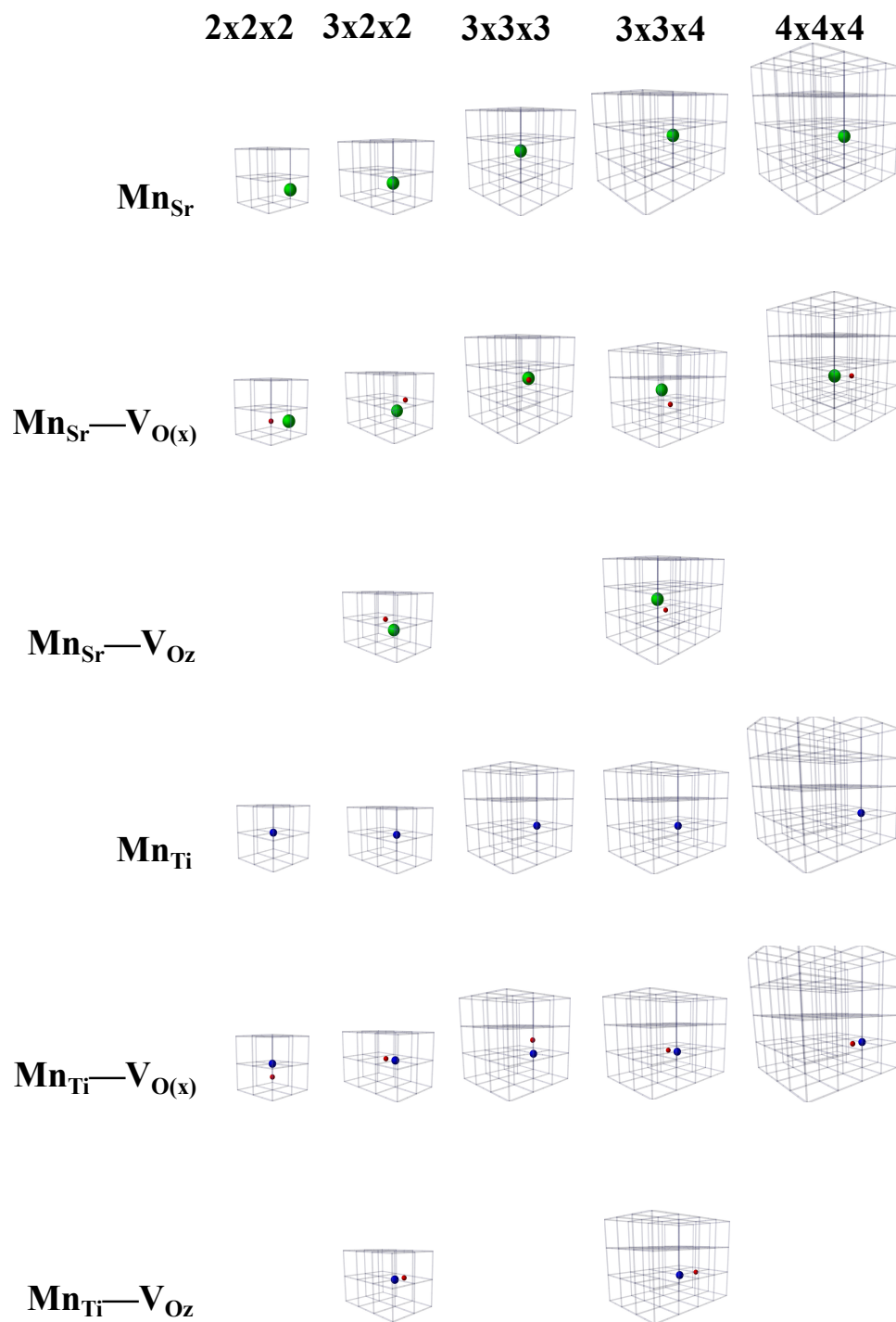


Fig. S4: Location of Mn and vacancies after optimization with the BLYP functional in QuantumEspresso.

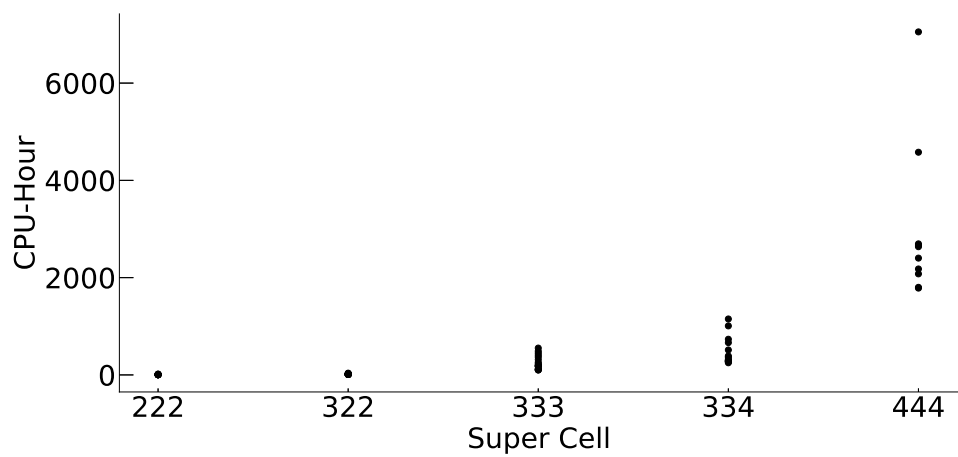
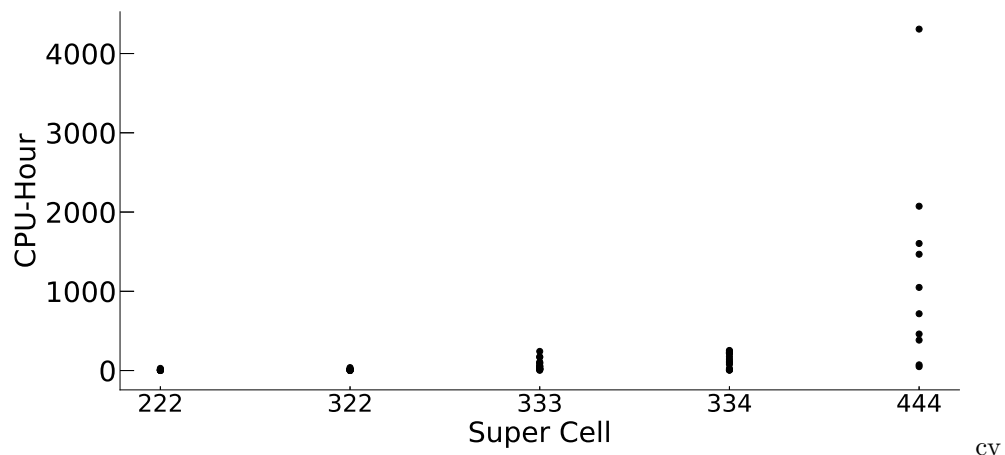


Fig. S5: Calculation time for single point energy calculation with the HSE06 functional in VASP.

Table S3: Final Energy/Atom from BLYP SCF Optimizations (eV)

	222	322	333	334	444
V_{Sr}	-744.2657762	-745.2385766	-746.3066162	-746.5311086	-746.8073023
V_{Ti}	-724.3104427	-732.0574714	-740.5011067	-742.1759561	-744.3691788
$V_{O(x)}$	-755.6305339	-752.7624734	-749.6372671	-749.0168518	-748.2032369
V_{Oz}		-752.7665551		-749.0168518	
$V_{Sr} - V_{O(x)}$	-752.9134956	-750.9311597	-748.8086861	-748.3950758	-747.8562941
$V_{Sr} - V_{Oz}$		-750.9229963		-748.3937153	
$V_{Ti} - V_{O(x)}$	-732.4955717	-737.5350859	-742.9705231	-744.0303994	-745.4113678
$V_{Ti} - V_{Oz}$		-737.5486915		-744.0317599	
Mn_{Sr}	-795.7684145	-779.6212884	-761.5748206	-757.9870238	-753.2468328
$Mn_{Sr} - V_{O(x)}$	-805.6011816	-785.803673	-764.1721296	-759.906774	-754.3175935
$Mn_{Sr} - V_{Oz}$		-785.7887069		-759.9081346	
Mn_{Ti}	-776.4348569	-766.721819	-755.8563869	-753.6890148	-750.8359205
$Mn_{Ti} - V_{O(x)}$	-785.7805435	-772.6905958	-758.410158	-755.5829143	-751.8903545
$Mn_{Ti} - V_{Oz}$		-772.6905958		-755.5815538	
Mn_{Sr}^{+2}			-761.4101928		
Mn_{Sr}^{+3}			-761.4999898		
$Mn_{Sr}^{+2} - V_O$			-764.010223		
$Mn_{Sr}^{+3} - V_O$			-764.1000199		
Mn_{Ti}^{+2}			-755.6822352		
Mn_{Ti}^{+3}			-755.769311		
$Mn_{Ti}^{+2} - V_O$			-758.2305641		
$Mn_{Ti}^{+3} - V_O$			-758.3176399		
<i>Pure</i>	-747.0168286	-747.0685298	-747.1433606	-747.1501634	-747.1610479

Table S4: BLYP Formation Energies (eV)

	222	322	333	334	444
V_{Sr}	28.793	31.629	37.822	37.388	40.072
V_{Ti}	102.809	110.573	121.703	125.306	129.34
$V_{O(x)}$	-25.686	-25.445	-22.919	-22.709	-20.827
V_{Oz}		-25.632		-22.574	
$V_{Sr} - V_{O(x)}$	7.608	10.128	15.433	16.471	17.975
$V_{Sr} - V_{Oz}$		10.563		16.657	
$V_{Ti} - V_{O(x)}$	79.277	88.385	97.961	101.796	106.912
$V_{Ti} - V_{Oz}$		87.613		101.647	
Mn_{Sr}	-79.046	-87.973	-87.748	-92.759	-92.42
$Mn_{Sr} - V_{O(x)}$	-103.549	-109.626	-110.115	-114.157	-116.073
$Mn_{Sr} - V_{Oz}$		-108.78		-114.214	
Mn_{Ti}	-9.958	-12.636	-9.632	-10.556	-9.459
$Mn_{Ti} - V_{O(x)}$	-34.793	-34.61	-31.86	-31.454	-30.591
$Mn_{Ti} - V_{Oz}$		-34.645		-31.394	
Mn_{Sr}^{+2}			-14.747		
Mn_{Sr}^{+3}			-46.521		
$Mn_{Sr}^{+2} - V_O$			-37.692		
$Mn_{Sr}^{+3} - V_O$			-69.244		
Mn_{Ti}^{+2}			64.556		
Mn_{Ti}^{+3}			33.114		
$Mn_{Ti}^{+2} - V_O$			42.946		
$Mn_{Ti}^{+3} - V_O$			11.637		

Table S5: HSE06 Energy Per Atom (eV)

	222	322	333	334	444
V_{Sr}	-198.0148511	-202.112484	-206.5867829	-207.4845842	-208.642966
V_{Ti}	-208.4336437	-209.012022	-209.6199424	-209.7471407	-209.9164343
$V_{O(x)}$	-214.5764628	-213.0668738	-211.4267926	-211.1000003	-212.6232848
V_{Oz}		-213.071719		-211.0989248	
$V_{Sr} - V_{O(x)}$	-202.331468	-205.0162594	-207.8961848	-208.4603362	-209.1977631
$V_{Sr} - V_{Oz}$		-205.0084437		-208.4593437	
$V_{Ti} - V_{O(x)}$	-213.0702195	-212.036507	-210.9618343	-210.748737	-210.474778
$V_{Ti} - V_{Oz}$		-212.050635		-210.7500737	
Mn_{Sr}	-200.8934164	-203.9852221	-207.3817383	-208.0744695	-208.971549
$Mn_{Sr} - V_{O(x)}$	-205.2288125	-206.8794141	-208.6840937	-209.0587394	-209.5232516
$Mn_{Sr} - V_{Oz}$		-206.8746108		-209.0583626	
Mn_{Ti}	-211.1545334	-210.8026532	-210.4345089	-210.3551869	-212.1997876
$Mn_{Ti} - V_{O(x)}$	-215.6819792	-213.7956101	-211.745963	-211.3379666	-212.7175917
$Mn_{Ti} - V_{Oz}$		-213.8005991		-211.3456746	
Mn_{Sr}^{+2}			-207.3027308		
Mn_{Sr}^{+3}			-207.3488361		
$Mn_{Sr}^{+2} - V_O$			-208.6065772		
$Mn_{Sr}^{+3} - V_O$			-208.6483583		
Mn_{Ti}^{+2}			-210.3467951		
Mn_{Ti}^{+3}			-210.4026405		
$Mn_{Ti}^{+2} - V_O$			-211.6685291		
$Mn_{Ti}^{+3} - V_O$			-211.7272356		
<i>Pure</i>	-209.985323	-210.023776	-210.0979741	-210.1057988	-210.1189973

Table S6: Coordination Number

	222	322	333	334	444
Mn_{Sr}	4.501	4.661	4.735	4.631	4.685
$Mn_{Sr} - V_{O(x)}$	4.455	4.475	4.496	4.463	4.778
$Mn_{Sr} - V_{Oz}$		4.477		4.457	
Mn_{Ti}	4.912	4.805	5.023	4.934	4.988
$Mn_{Ti} - V_{O(x)}$	4.749	4.778	4.796	4.816	5.116
$Mn_{Ti} - V_{Oz}$		4.907		5.109	
Mn_{Sr}^{+2}			4.757		
Mn_{Sr}^{+3}			4.442		
$Mn_{Sr}^{+2} - V_O$			4.155		
$Mn_{Sr}^{+3} - V_O$			4.17		
Mn_{Ti}^{+2}			5.249		
Mn_{Ti}^{+3}			4.93		
$Mn_{Ti}^{+2} - V_O$			5.046		
$Mn_{Ti}^{+3} - V_O$			4.966		

Table S7: Atomic identities at high symmetry points in supercells

Supercell	High Symmetry Point	Atom
222	Γ	Ti
	M	Ti
	X	Ti
	R	Ti
322	Γ	O
	M	Ti
	X	Ti
	A	Ti
	Z	O
	R	Ti
333	Γ	Sr
	M	O
	X	A-Cell Face Center
	R	Ti
334	Γ	A-Cell Face Center
	M	O
	X	A-Cell Face Center
	A	Ti
	Z	O
	R	O
444	Γ	Ti
	M	Ti
	X	Ti
	R	Ti

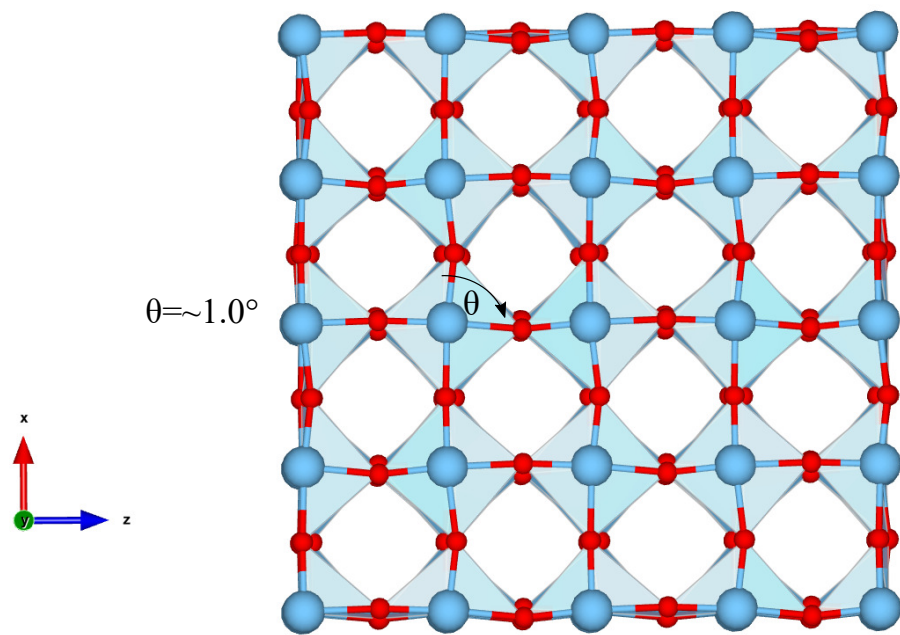


Fig. S6: Antiferrodistortive-like rotations in 4 x 4 x 4 $V_{Sr}-V_O$

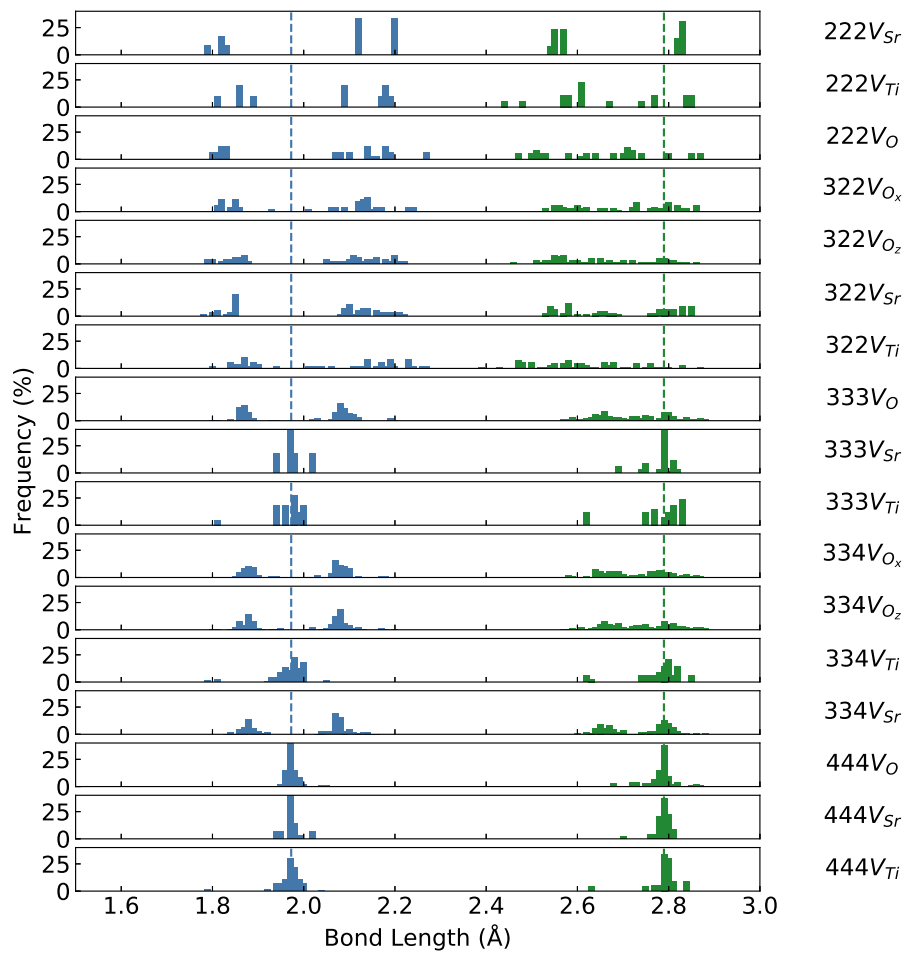


Fig. S7: Histogram of Sr-O bond lengths (green) and Ti-O bond lengths (blue) in singly defected cells. The bulk value is represented by the vertical dashed line.

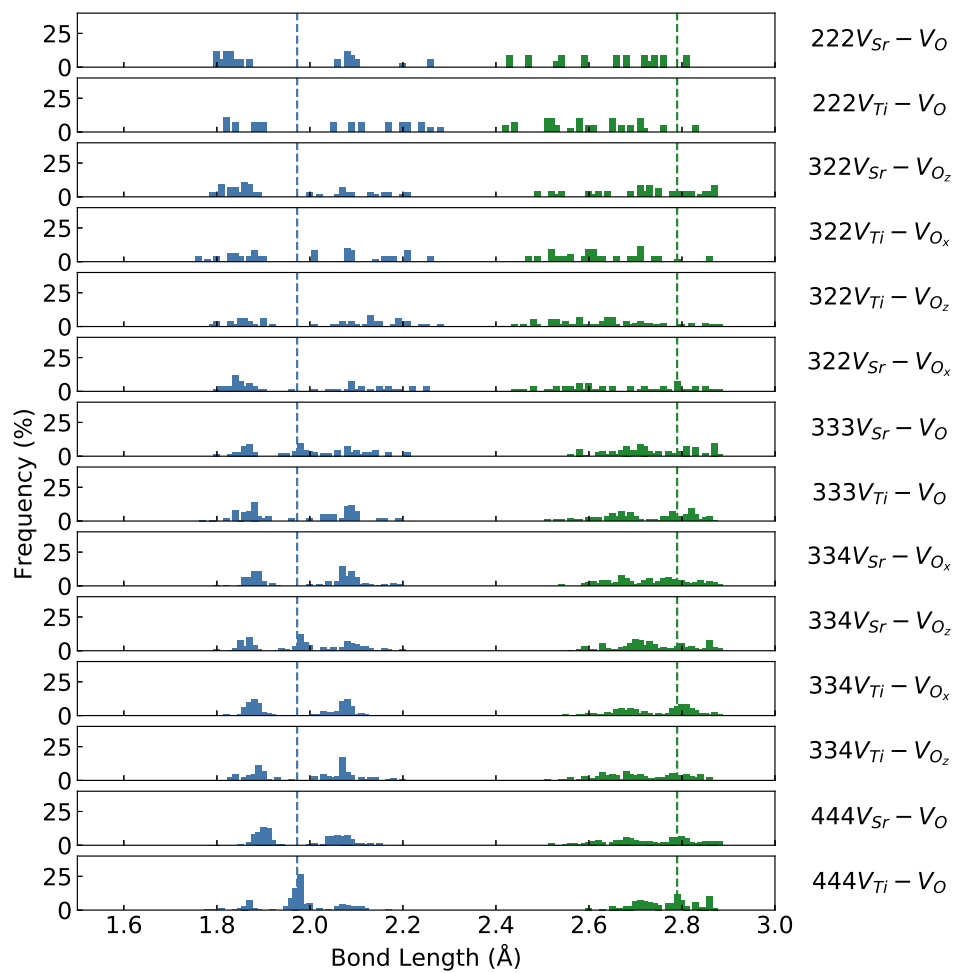


Fig. S8: Histogram of Sr-O bond lengths (green) and Ti-O bond lengths (blue) in doubly defected cells. The bulk value is represented by the vertical dashed line.

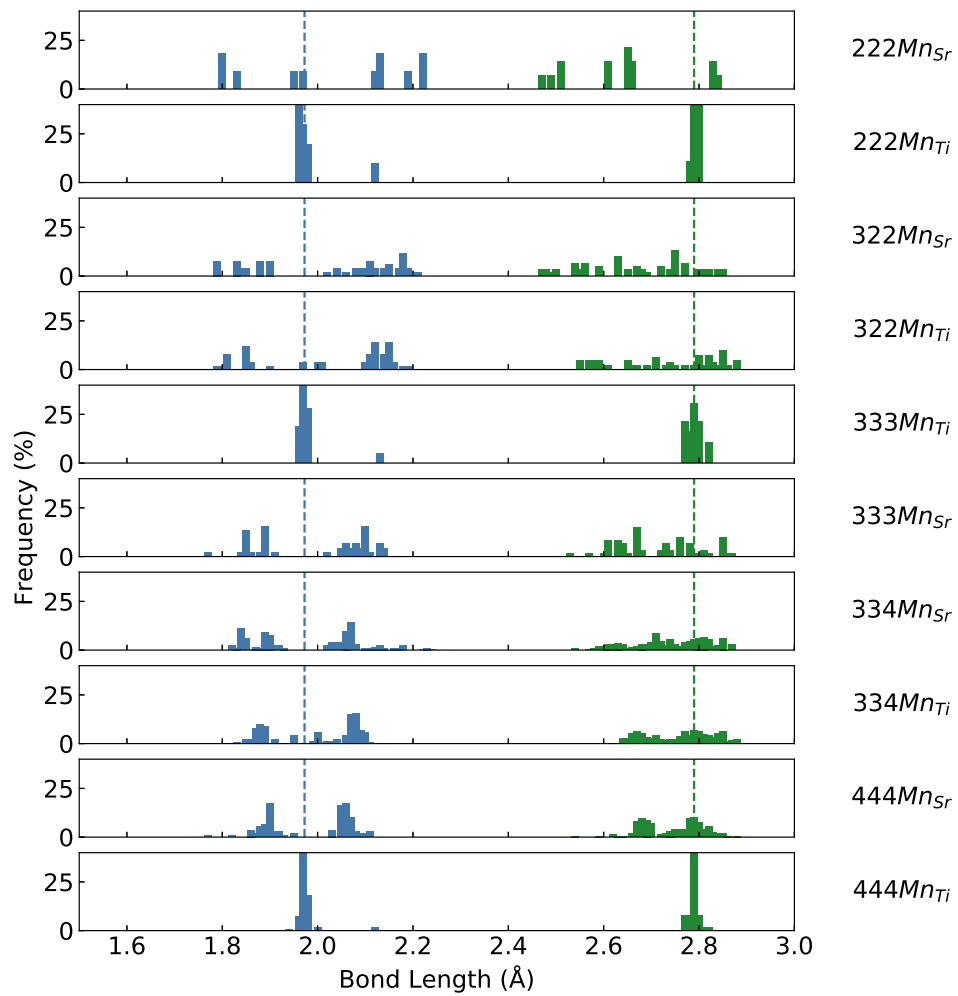


Fig. S9: Histogram of Sr-O bond lengths (green) and Ti-O bond lengths (blue) in singly Mn-doped defected cells. The bulk value is represented by the vertical dashed line.

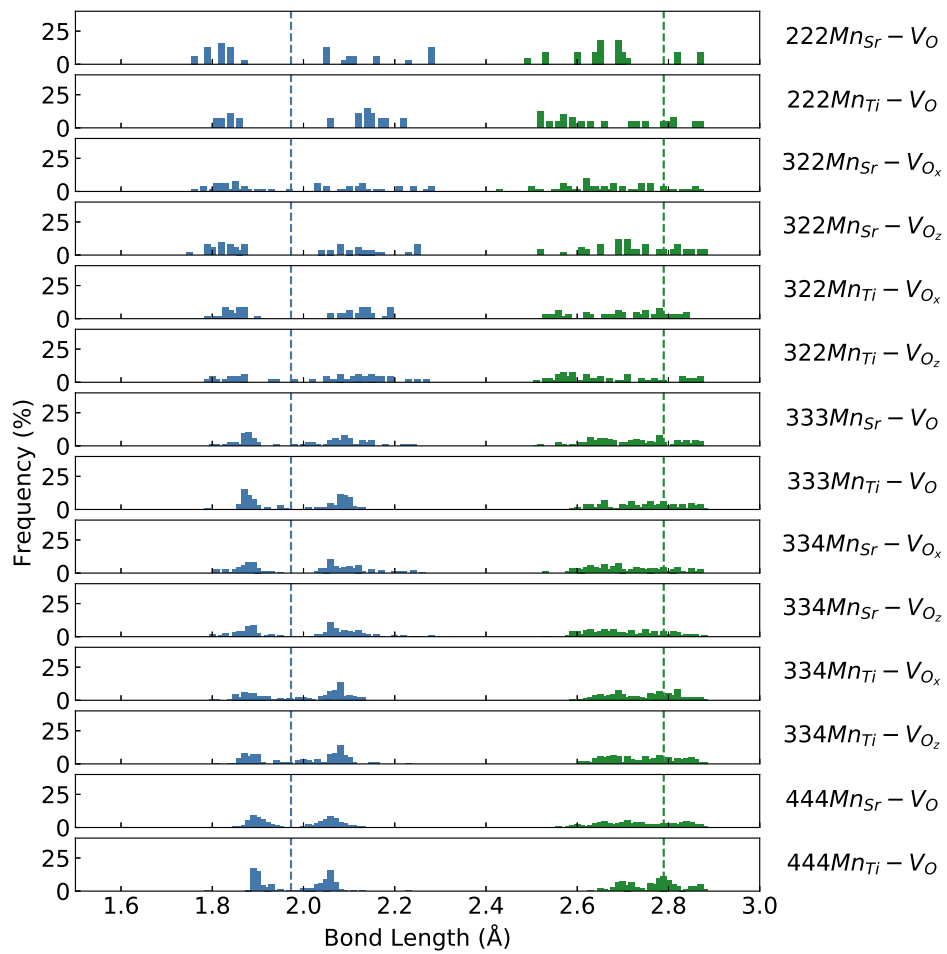


Fig. S10: Histogram of Sr-O bond lengths (green) and Ti-O bond lengths (blue) in singly defected cells. The bulk value is represented by the vertical dashed line.

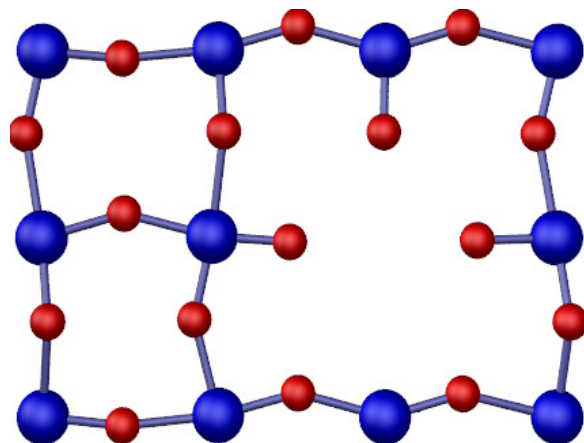


Fig. S11: $3 \times 2 \times 2$ $V_{Ti}-V_{Oz}$ supercell capturing octahedral tilt.

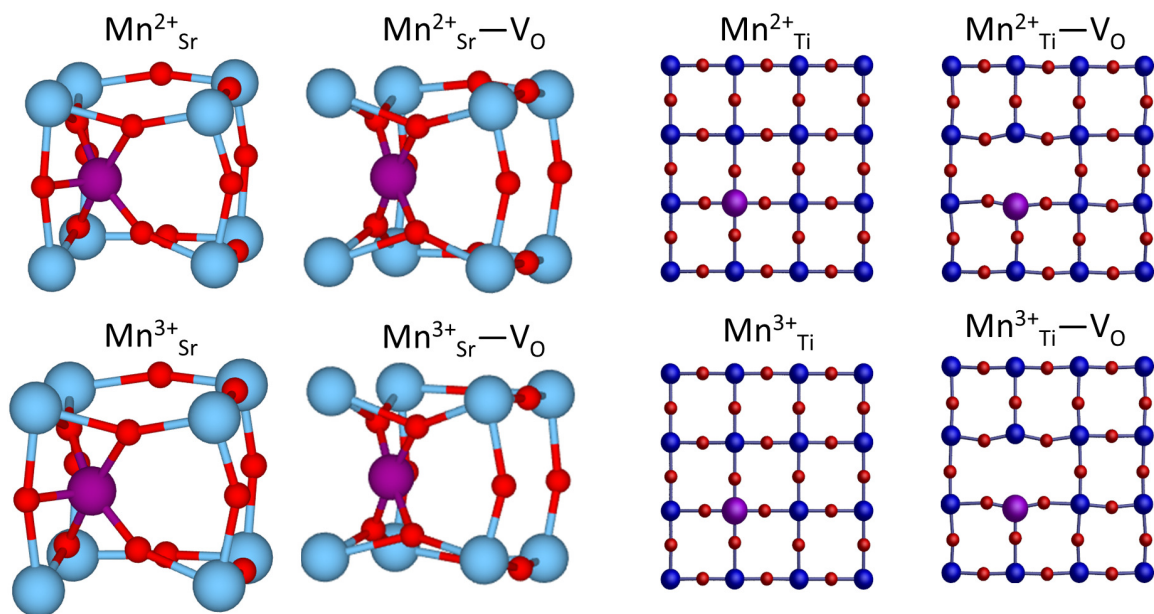


Fig. S12: Geometries predicted for $Mn^{2+/3+}$ dopants

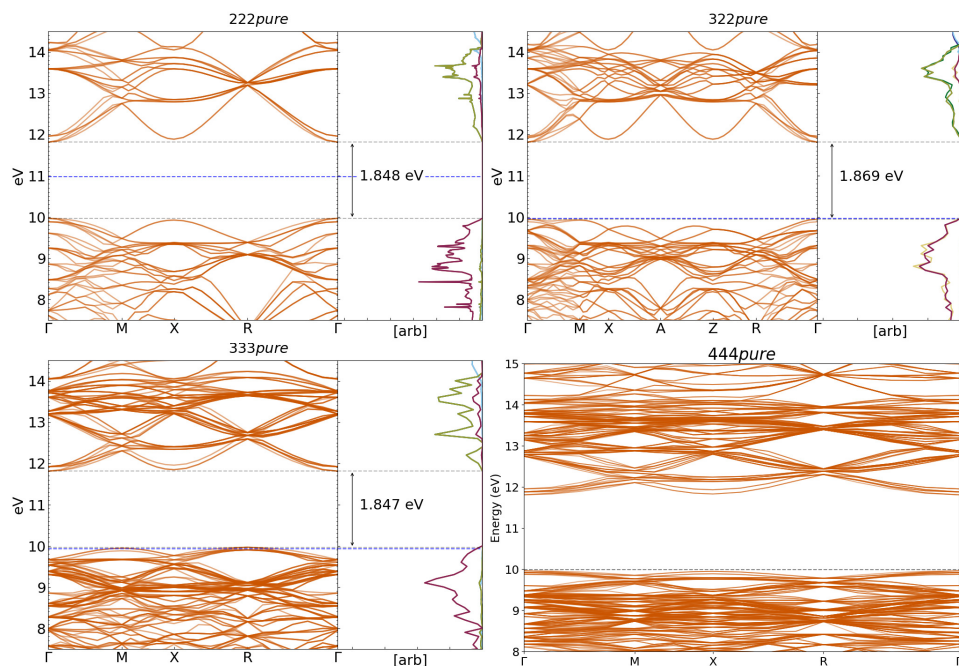


Fig. S13: BLYP predicted bands for selected undefected supercells

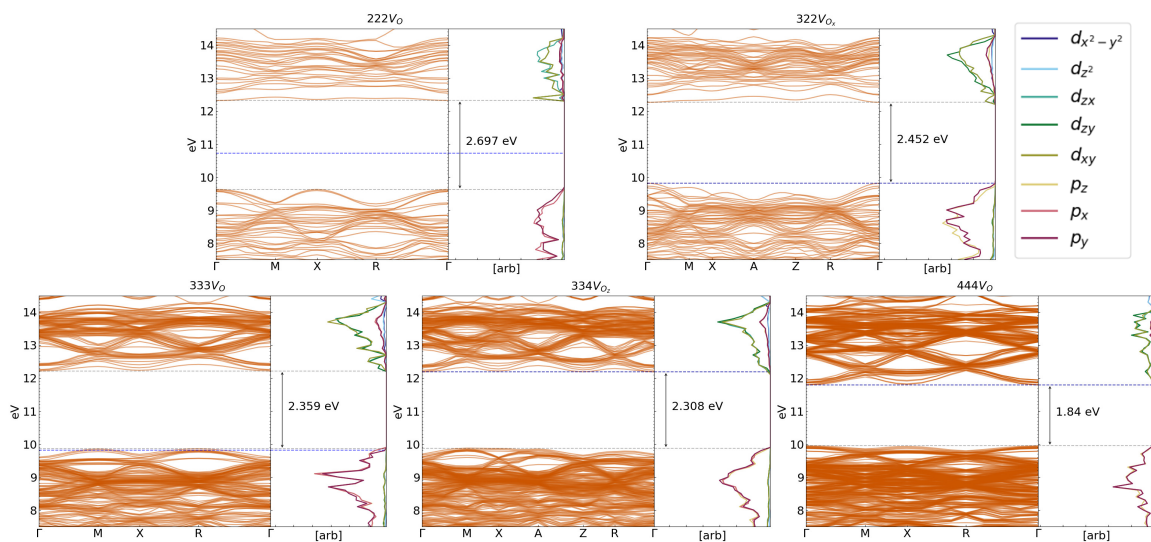


Fig. S14: BLYP predicted bandstructures for V_O supercells

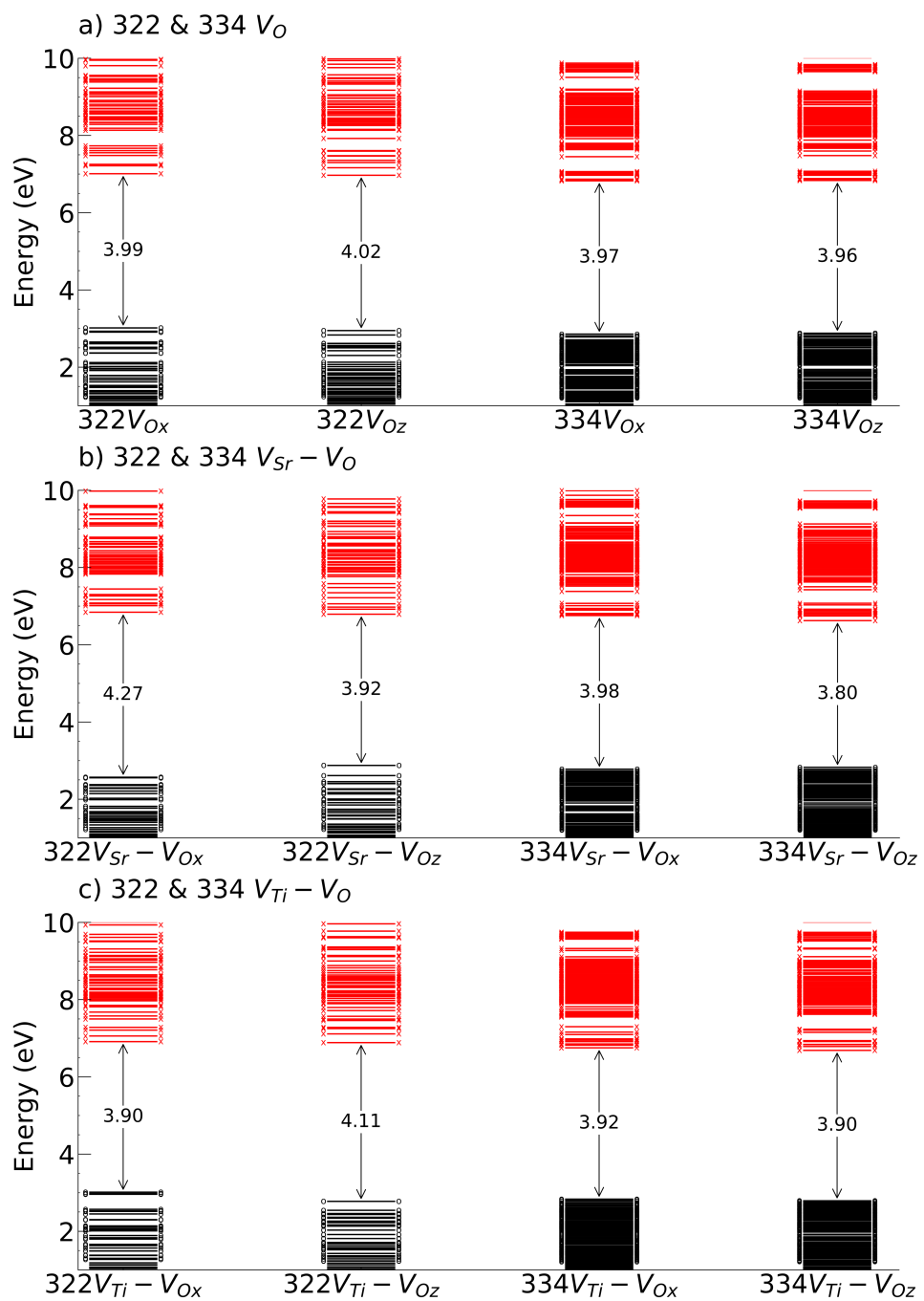


Fig. S15: HSE06 band structures for asymmetric V_O defects.

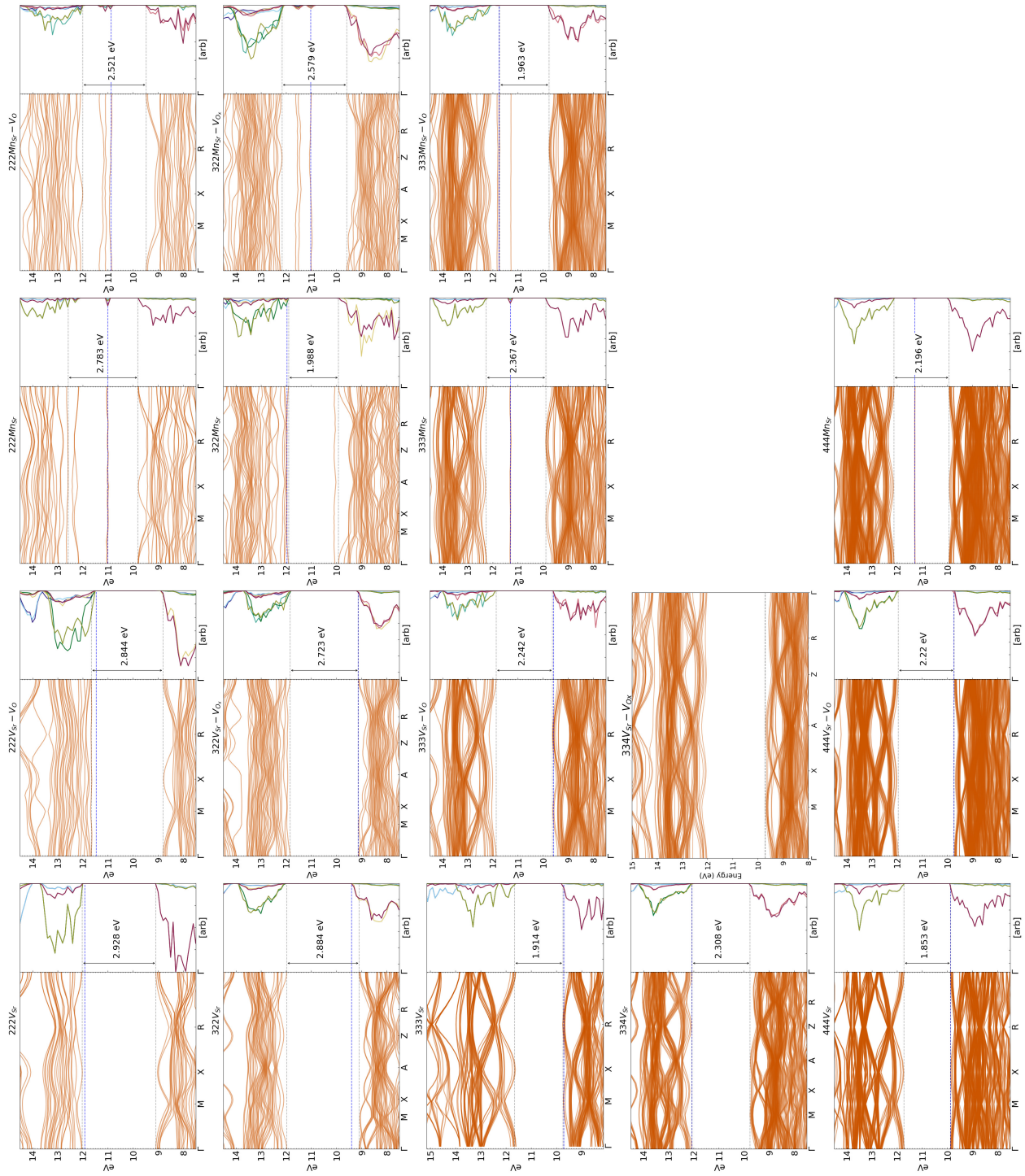


Fig. S16: BLYP band structures for A-site defects

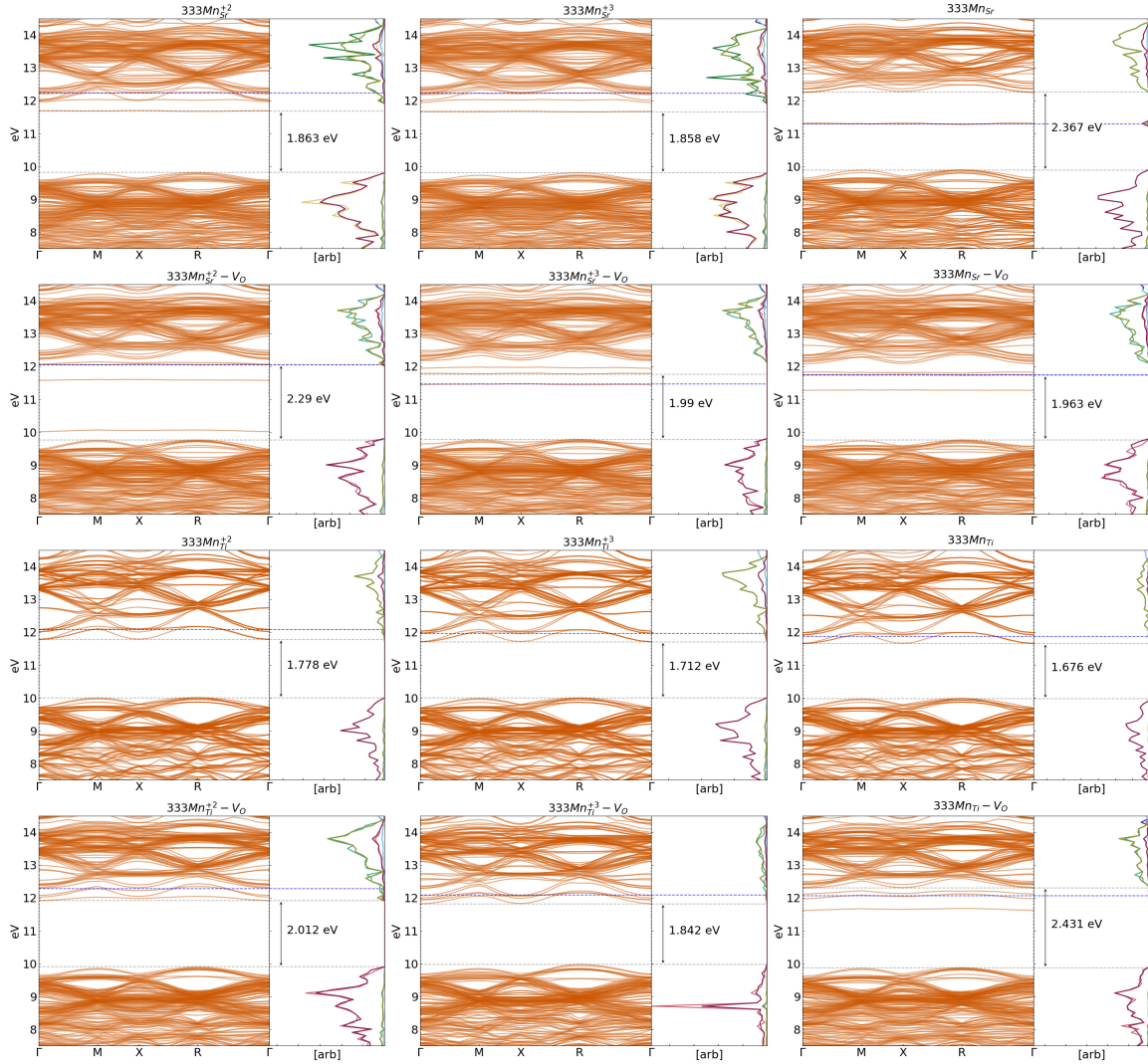


Fig. S17: BLYP band structures for $\text{Mn}^{2+/3+/4+}$ defects.

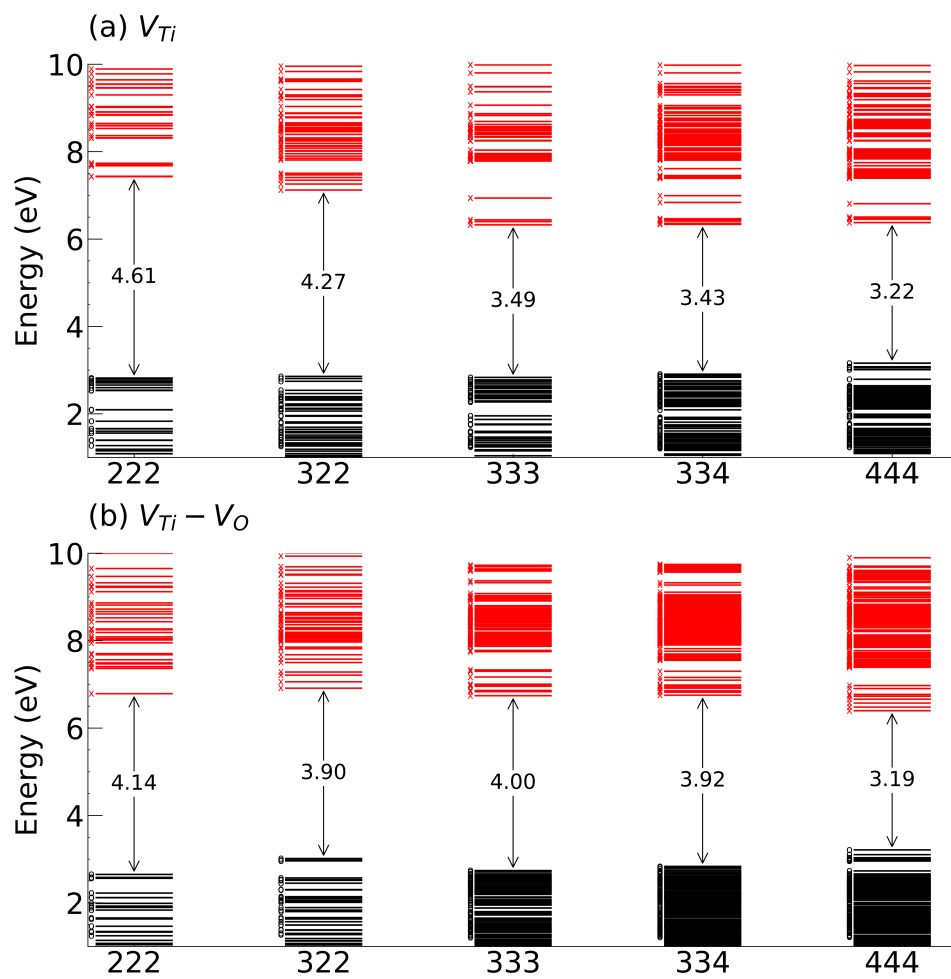


Fig. S18: HSE06 predicted energy levels for V_{Ti} defects.

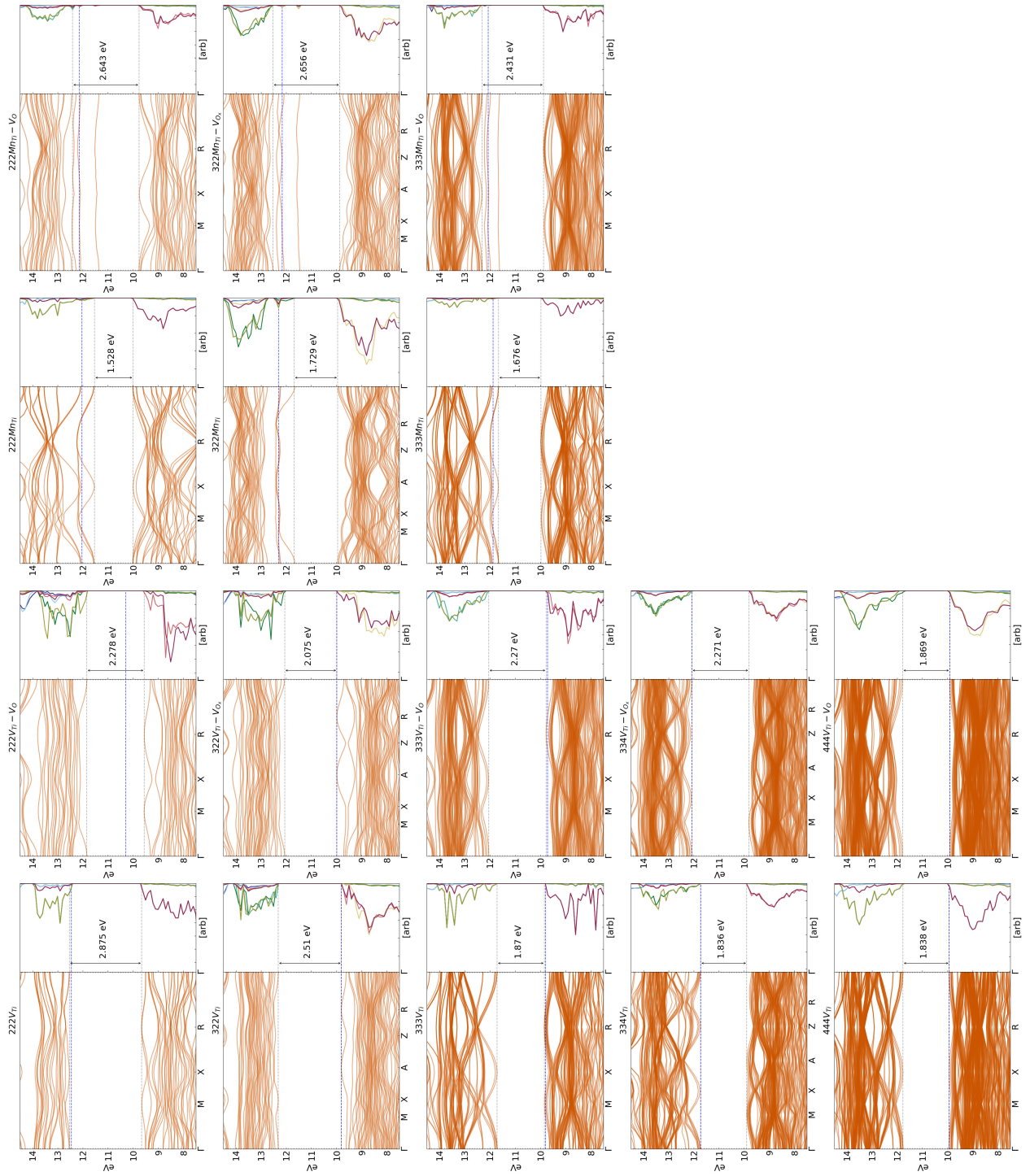


Fig. S19: BLYP bands structures for Mn^{2+/3+/4+} defects.

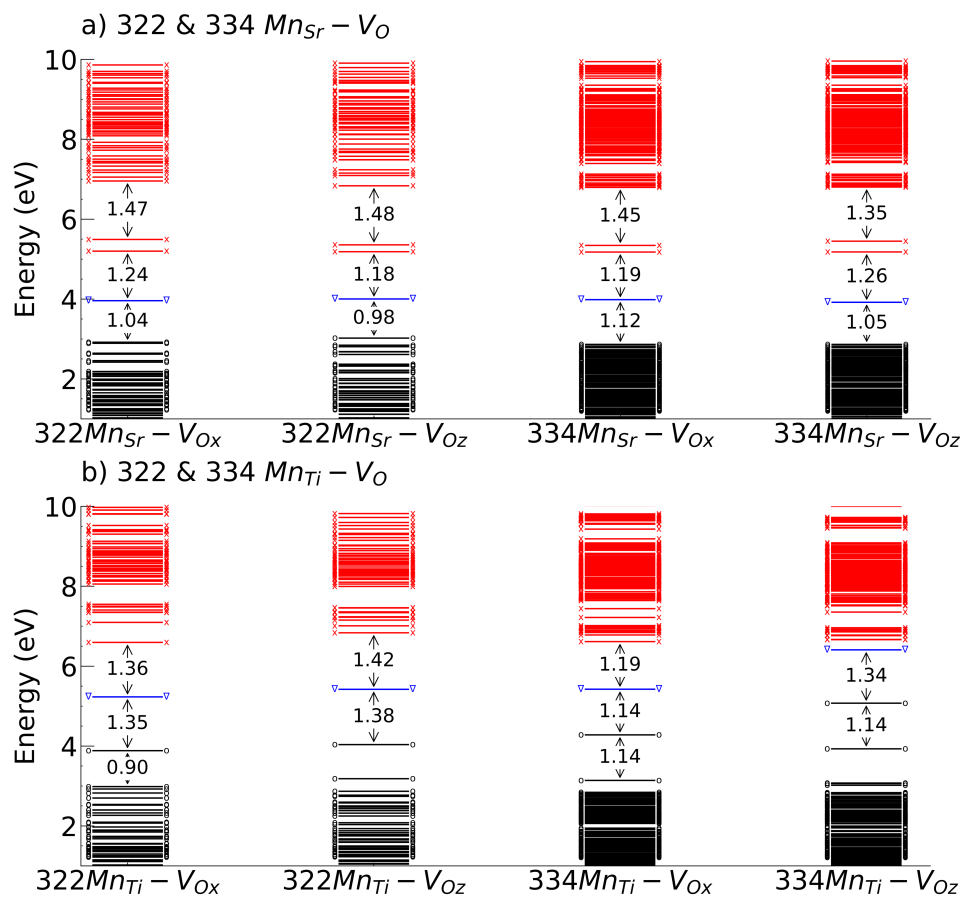


Fig. S20: HSE06 predicted energy levels for asymmetric Mn-doped supercells